ISSN 1674-1056
http://cpb.iphy.ac.cn
http://iopscience.iop.org/cpb
中国物理 B
Chinese Physics
中国物理
Chinese Physics B

The effect of Mn-doped ZnSe passivation layer on the performance of CdS/CdSe quantum dot-sensitized solar cells

Yun-Long Deng(邓云龙), Zhi-Yuan Xu(徐知源), Kai Cai(蔡凯), Fei Ma(马飞), Juan Hou(侯娟), Shang-Long Peng(彭尚龙)
Citation: Chin. Phys. B . 2019, 28(9): 098802 . **doi:** 10.1088/1674-1056/28/9/098802
Journal homepage: http://cpb.iphy.ac.cn; http://iopscience.iop.org/cpb

What follows is a list of articles you may be interested in

Exploring alkylthiol additives in PBDB-T:ITIC blended active layers for solar cell applications

Xiang Li(李想), Zhiqun He(何志群), Mengjie Sun(孙盟杰), Huimin Zhang(张慧敏), Zebang Guo(郭泽邦), Yajun Xu(许亚军), Han Li(李瀚), Chunjun Liang(梁春军), Xiping Jing(荆西平)
Chin. Phys. B . 2019, 28(8): 088802 . **doi:** 10.1088/1674-1056/28/8/088802

Effect of carrier mobility on performance of perovskite solar cells

Yi-Fan Gu(顾一帆), Hui-Jing Du(杜会静), Nan-Nan Li(李楠楠), Lei Yang(杨蕾), Chun-Yu Zhou(周春宇)
Chin. Phys. B . 2019, 28(4): 048802 . **doi:** 10.1088/1674-1056/28/4/048802

Detection of finger interruptions in silicon solar cells using photoluminescence imaging

Lei Zhang(张磊), Peng Liang(梁鹏), Hui-Shi Zhu(朱慧时), Pei-De Han(韩培德)
Chin. Phys. B . 2018, 27(6): 068801 . **doi:** 10.1088/1674-1056/27/6/068801

Application of millimeter-sized polymer cylindrical lens array concentrators in solar cells

Yao-Ju Zhang(张耀举), Yi-Jie Li(李艺杰), Jie Lin(林洁), Chao-Long Fang(方朝龙), Si-Yuan Liu(刘思远)
Chin. Phys. B . 2018, 27(5): 058801 . **doi:** 10.1088/1674-1056/27/5/058801

Efficient ternary organic solar cells with high absorption coefficient DIB-SQ as the third component

Hui-Xin Qi(齐慧欣), Bo-Han Yu(余泊含), Sai Liu(刘赛), Miao Zhang(张苗), Xiao-Ling Ma(马晓玲), Jian Wang(王健), Fu-Jun Zhang(张福俊)
Chin. Phys. B . 2018, 27(5): 058802 . **doi:** 10.1088/1674-1056/27/5/058802

SPECIAL TOPIC — 110th Anniversary of Lanzhou University

The effect of Mn-doped ZnSe passivation layer on the performance of CdS/CdSe quantum dot-sensitized solar cells*

Yun-Long Deng(邓云龙)[1], Zhi-Yuan Xu(徐知源)[1], Kai Cai(蔡凯)[1], Fei Ma(马飞)[1,†], Juan Hou(侯娟)[2], and Shang-Long Peng(彭尚龙)[1,‡]

[1] National & Local Joint Engineering Laboratory for Optical Conversion Materials and Technology, School of Physical Science and Technology, Lanzhou University, Lanzhou 730000, China

[2] College of Science, Key Laboratory of Ecophysics, Department of Physics, Shihezi University, Shihezi 832003, China

(Received 31 May 2019; revised manuscript received 11 July 2019; published online 23 August 2019)

ZnSe as a surface passivation layer in quantum dot-sensitized solar cells plays an important role in preventing charge recombination and thus improves the power conversion efficiency (PCE). However, as a wide bandgap semiconductor, ZnSe cannot efficiently absorb and convert long-wavelength light. Doping transition metal ions into ZnSe semiconductors is an effective way to adjust the band gap, such as manganese ions. In this paper, it is found by the method of density functional theory calculation that the valence band of ZnSe moves upward with manganese ions doping, which leads to acceleration of charge separation, wider light absorption range, and enhancing light harvesting. Finally, by using ZnSe doped with manganese ions as the passivation layer, the TiO_2/CdS/CdSe co-sensitized solar cell has a PCE of 6.12%, and the PCE of the solar cell increases by 9% compared with the undoped one (5.62%).

Keywords: solar cells, passivation layer, manganese ions, doping

PACS: 88.40.hj, 88.40.H–, 81.07.Ta **DOI:** 10.1088/1674-1056/ab37f3

1. Introduction

Developing low-cost and high-performance solar energy devices that reduce reliance on fossil energy has become an urgent issue in the world.[1] Quantum dot-sensitized solar cells (QDSSCs) attracted much attention of researchers because of their simple fabrication process, low manufacturing cost, and theory power conversion efficiency (PCE) more than 44%.[2–4] However, due to the tiny size and large relative surface area of conventional quantum dot sensitizers, there are many defects in the photoanode interface.[5,6] These surface defects lead to strong electron–hole recombination, which seriously limits the power conversion efficiency of QDSSCs.[7,8] It is an effective method to improve the PCE of QDSSCs by preparing a passivation layer on the surface of quantum dots to reduce surface defects.[9–12] Meanwhile, Huang *et al.* pointed out that both the conduction band position and the valence band position of ZnSe were higher than CdS/CdSe quantum dots.[13] Therefore, the type-II core–shell structure with quantum dots not only can effectively prevent the reverse transmission of photoelectrons to the electrolyte, but also facilitate the rapid transport of holes from the quantum dots to the electrolyte after the exciton separation.[14] Many studies have shown that devices with ZnSe as a passivation layer have excellent performance.[15–17] However, ZnSe with wide bandgap does not allow absorption in long wavelength regions.[18]

Doping transition metal ions is an effective method to adjust the energy band structure of semiconductor materials, such as manganese ions.[19,20] Doping ions will directly affect the density distribution of the electronic states in the semiconductor, thereby affecting the properties of the nanomaterials.[13] The influence of the doped manganese ions on quantum dots has been widely reported.[21] Kamat *et al.* firstly doped manganese ions into CdS/CdSe quantum dots, and finally improved the PCE of QDSSC to 5%.[22] Cao's team also improved the PCE of CdSe QDSSC to over 6% by means of optimization of the doping process.[23] In particular, Gopi *et al.* studied the effect of manganese ions doping on ZnSe surface, and obtained 5.67% conversion efficiency through this method, which greatly improved the PCE of CdS/CdSe QDSSCs.[22] So far, less work has been done to study the effect of Mn ions on CdS/CdSe QDSSCs from the aspect of electronic band structure, which is the key to photoelectric properties of devices and the process of electron hole separation.[13] The research on the influence of manganese ions on the electronic band structure is conducive to deepening the understanding of charge generation, transmission, and recombina-

*Project supported by the National Natural Science Foundation of China (Grant Nos. 61376011, 61704114, 51402141, and 61604086), the Gansu Provincial Natural Science Foundation, China (Grant No. 17JR5RA198), the Fundamental Research Funds for the Central Universities, China (Grant Nos. lzujbky-2018-119 and lzujbky-2018-ct08), and the Fund from Shenzhen Science and Technology Innovation Committee, China (Grant No. JCYJ20170818155813437), and the Key Areas Scientific and Technological Research Projects in Xinjiang Production and Construction Corps (Grant No. 2018AB004).

†Corresponding author. E-mail: maf@lzu.edu.cn

‡Corresponding author. E-mail: pengshl@lzu.edu.cn

© 2019 Chinese Physical Society and IOP Publishing Ltd

tion mechanisms in QDSSCs system.[16,17]

In this work, we investigate the effect of manganese ions-doped ZnSe on CdS/CdSe co-sensitized solar cells. The doping of manganese ions affects the distribution of electron state density in quantum dots and thus changes the energy band structure of ZnSe nanomaterials. Compared with ZnSe passivated CdS/CdSe QDSSCs, manganese ions-doped ZnSe as a passivation layer significantly improves the light absorption and reduces interfacial recombination of the solar cells, thus enhancing the short circuit current density J_{sc}. The results show that the PCE of the device was 6.12%, and the PCE was increased by 9% compared with the undoped one (5.62%).

2. Experimental technology

2.1. Synthesis of the passivation layer

We prepared TiO_2/CdS/CdSe film on FTO glass according to the previous method.[23] Then, the ZnSe and Mn-doped ZnSe layers were prepared by SILAR method. Specifically, 0.048-mol·L^{-1} Zn $(Ac)_2{\cdot}2H_2O$ and 0.012-mol·L^{-1} Mn $(Ac)_2{\cdot}4H_2O$ were mixed into a homogeneous solution for later use. Then, the TiO_2/CdS/CdSe films without passivation were soaked in the mixed solution and 0.06-mol·L^{-1} NaHSe for 2 min respectively. After each deposition, the excess solution on the surface of the TiO_2/CdS/CdSe film should be washed clean with deionized water. A total of three SILAR cycles are required to form uniform Mn–ZnSe passivation layers. NaHSe is formed by mixing $NaBH_4$ with selenium powder in deionized water in an atmosphere of argon. ZnSe layer was prepared by the same synthesis process using 0.06 mol·L^{-1} Zn $(Ac)_2{\cdot}2H_2O$ solution instead of the mixed solution containing zinc ions and manganese ions. The preparation method of electrolyte and counter electrode is the same as our previous work, and the device is finally assembled into a sandwich structure.[23]

2.2. Characterization

The micro-morphologies of the photoanodes were researched by field emission scanning electron microscopy (FE-SEM, Hitachi S-4800). The chemical composition of the sample was analyzed by x-ray photoelectron spectroscopy (XPS, Kratos AXIS UltraDLD, UK). The UV-visible (UV-Vis) light absorption spectrum of the photoanode was measured by UV-visible spectrophotometer (Hitachi U-3900H, Japan). The *J*–*V* curves were measured (Keithley 2400 source meter) under a solar illuminance (100 mW·cm^{-2}, AM1.5G, Zolix, China).

3. Results and discussion

3.1. Characterization of photoanodes

Figure 1(a) shows an SEM image of the ZnSe-passivated photoanode. In the SEM image, the ZnSe passivation layer is clearly visible on the surface of the TiO_2 substrate, and these TiO_2 particles have a size of about 25 nm. The Mn-doped ZnSe passivation layer is shown in Fig. 1(b). The surface of the TiO_2 substrate is covered with a larger area of porous passivation film. These passivation films, having a pore structure, can improve the penetration of the electrolyte and have a light reflection effect. The possible reason is that Mn ions act as a nucleation center to promote the growth of ZnSe films.[24] Figure 1(c) shows the main components of the photoanodes by EDX. The atomic percentage of EDX is listed in Table A1 in Appendix A, combined with the EDX spectra of TiO_2/CdS/CdSe/ZnSe samples as shown in Fig. A1, and a small amount of Mn (1.29%) was introduced into the sample. Figure 1(d) shows the XPS spectrum of Mn-doped ZnSe films grown on the TiO_2/CdS/CdSe photoanodes. The binding energy of 284.6 eV corresponds to the C 1s peak for calibration. The binding energies of 641 eV and 652 eV correspond to $2p_{3/2}$ and $2p_{1/2}$ of Mn, respectively as indicated by the red arrow in the figure. The Se 3d peak appears at a binding energy of 55 eV. Figure A2 shows the XPS spectra of Se with and without manganese ions doping. As shown in Fig. A2, the binding energy of the Se 3d peak for Mn–ZnSe shift at high binding energy, which may be caused by the interaction between doped Mn and Se.[25] Therefore, the introduction of Mn ions can be determined in conjunction with Fig. 1(c).

Taking the TiO_2/CdS/CdSe/ZnSe sample as a reference, the UV-visible curve from 350 nm to 750 nm of the Mn–ZnSe passivated photoanode is shown in Fig. 2. It shows that the sample treated with Mn–ZnSe passivation has significant improvement in light absorption intensity and red-shift. The enhanced light absorption intensity may be due to the introduction of more porous membrane structure, which increases light reflection and increases the utilization ratio of light.[26,27] At the same time, the red-shift of absorption edge is probably ascribed to the reduce of the forbidden band width by Mn ion doping into the semiconductor nanomaterial, which leads to the lower energy required for electrons to be excited to the conduction band.[28] This conclusion is discussed in detail in the next data.

In order to study the effect of Mn ions on the ZnSe band structure, the ZnSe and Mn–ZnSe band structures were calculated and analyzed. The calculation is done by Vienna *Ab initio* Simulation Package, namely VASP version 5.2 software. The code is mainly based on density functional theory (DFT). In the calculation, the generalized gradient approximation (GGA) of Perdew–Berk–Ernzerhof (PBE) is selected to

describe the electron exchange–correlation energy by the projector augmented wave (PAW) method, and the cutoff energy of the plane wave is selected as 400 eV.[21] ZnSe and Mn-doped ZnSe were calculated in unit cell (8 atoms) and supercell ($2\times2\times2$, 64 atoms), respectively. Structural optimization was achieved by relaxation of the positions of all atoms until the convergence difference of force on each atom was less than 0.01 eV·Å^{-1}.[29] It is worth mentioning that the doping concentration of Mn ions is 1/64 selected according to the experimental data, and the doping site is the place to replace Zn atom. According to the Monkhorst–Pack method, the structure optimization was divided into $5\times5\times5$ and $11\times11\times11$ in the Brillouin zone, and the lattice constants of Mn ion-doped ZnSe and undoped ZnSe were fixed at 11.45 Å and 5.74 Å. Gaussian smearing and *M*–*K*–*Γ*–*M* high symmetry points was used to calculate the band structure of Mn ions doped with change.

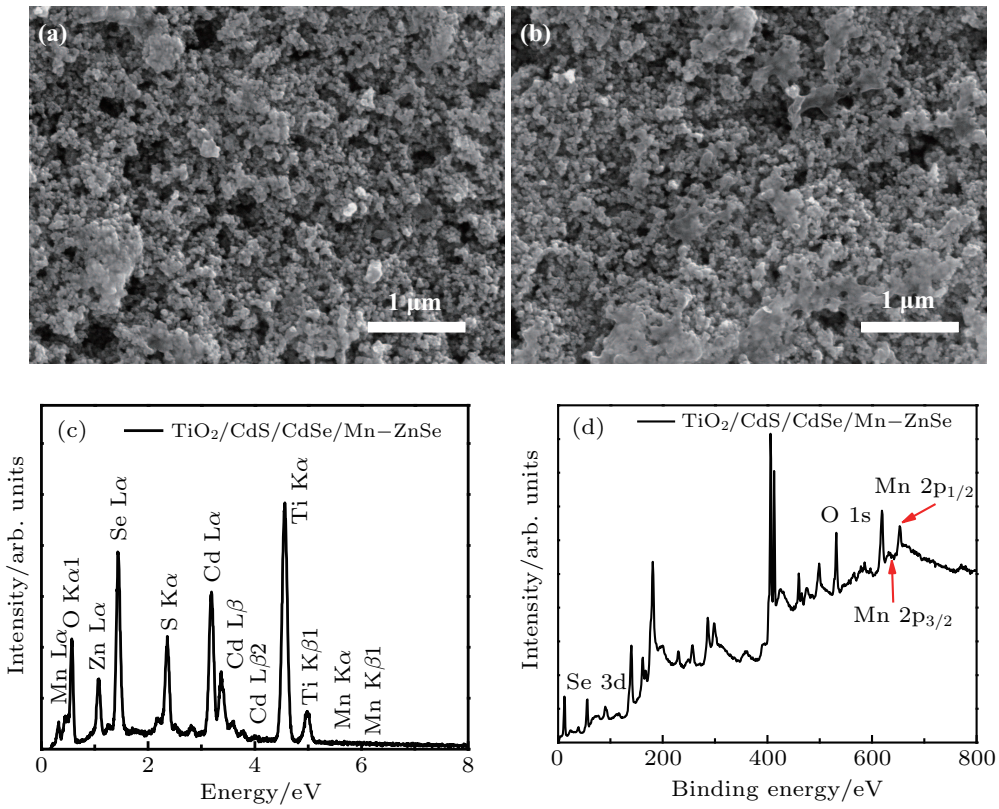


Fig. 1. Topside SEM of (a) TiO_2/CdS/CdSe/ZnSe and (b) TiO_2/CdS/CdSe/Mn–ZnSe photoanodes. (c) Energy dispersive x-ray spectrum of TiO_2/CdS/CdSe/Mn–ZnSe and (d) photoanodic x-ray photoelectron spectroscopy of TiO_2/CdS/CdSe/ Mn–ZnSe samples.

As shown in Fig. 3, pure ZnSe and Mn-doped ZnSe showed the property of band gap semiconductor materials. The band gaps of ZnSe and Mn-doped ZnSe are 1.14 eV and 0.89 eV, respectively. It means that ZnSe band gap width decreases after Mn ion doping. Because the Coulomb interaction is not considered accurately, the calculation results of forbidden band width based on DFT are often small, so the calculated value of forbidden band width of pure ZnSe (1.14 eV) is less than its true value (2.70 eV).[24] Therefore, we should pay more attention to the change of ZnSe bandgap before and after Mn ion doping, rather than the absolute calculated value of E_g.

The energy band arrangement diagram is shown in Fig. 4, where E_2 corresponds to the infrared absorption edge of the original undoped sample. As Mn is added, it causes the VBM of ZnSe to move up so that E_2' is less than E_2. In other words, the photoanode passivated by Mn-doped ZnSe will have a longer infrared absorption edge than the sample passivated by ZnSe. Combined with the calculation and analysis of UV-Vis and energy band structure, it can be concluded that it is the impurity Mn that causes the ZnSe valence band position to move up, thus causing the red-shift of the UV-Vis spectral line of the sample.[30]

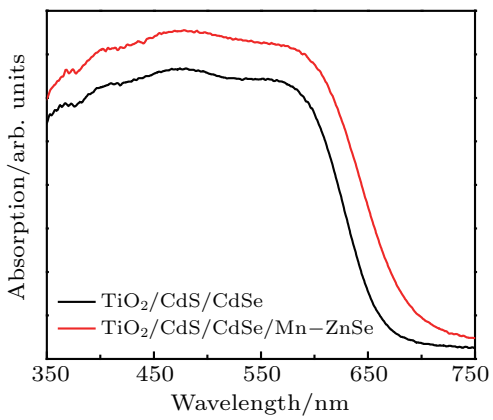


Fig. 2. UV-Vis absorption spectrum of photoanodes with and without Mn doping.

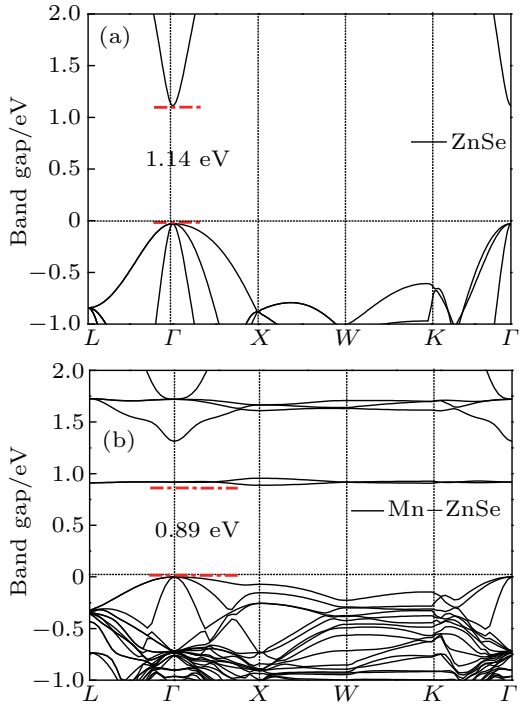


Fig. 3. Calculation energy band structure diagram of (a) ZnSe and (b) Mn-doped ZnSe.

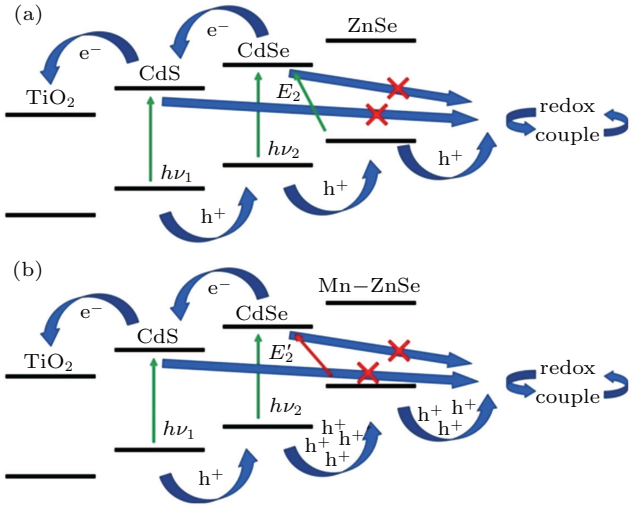


Fig. 4. Schematic diagram of the energy band position of (a) ZnSe and (b) Mn-doped ZnSe as a passivation layer.

3.2. Characterization of devices

The dark current curves of the two samples are shown in Fig. 5(a). The testing process is carried out with a scanning range of −0.1 V to 0.6 V and a point interval of 7 mV. It can be seen that the samples doped with Mn ions have lower dark current compared with the pure ZnSe passivation samples.[31] The passivation layer of Mn–ZnSe can effectively inhibit the charge recombination process near the surface of the photoanode, so it can be said that ZnSe doped with Mn ions has a better passivation effect. Incident photoelectron conversion efficiency (IPCE) can be used to estimate the light harvesting efficiency, charge injection efficiency, and charge collection efficiency of QDSSCs. Figure 5(b) shows the IPCE spectrum of devices with and without Mn ions. The J_{sc} results for IPCE integration are also shown in Fig. 5(b). It is worth noting that the device consisting of Mn ions-doped photoanode has a larger value than a sample without Mn ions doping, and the same is true for the integral J_{sc} value. As shown in Fig. 5(b), the integral J_{sc} values of the ZnSe and Mn-doped ZnSe samples are 15.28 mA·cm^{-2} and 17.1 mA·cm^{-2}, respectively, which are like the J_{sc} results of the *I*–*V* test in Table 1. Meanwhile, the Mn-doped sample showed a significant red-shift, which is consistent with the results of Fig. 2 and Fig. 3.

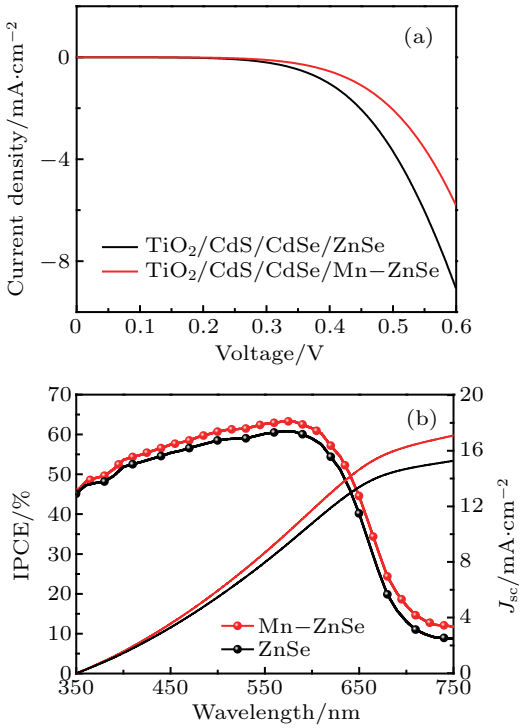


Fig. 5. (a) Dark current of ZnSe and Mn-doped ZnSe as a passivation layer. (b) IPCE spectra and integrated J_{sc}.

The IPCE value can be divided into three parts: light harvesting efficiency η_{LHE}, charge injection efficiency η_{Inj}, and charge collection efficiency η_{cc}, as shown in the following formula (1)[32]

$$\mathrm{IPCE} = \eta_{LHE} \times \eta_{Inj} \times \eta_{cc}, \tag{1}$$

where η_{LHE} is light harvesting efficiency, η_{Inj} is charge injection efficiency, and η_{cc} is charge collection efficiency. The light harvesting efficiency η_{LHE} is related to the light absorption intensity and can be derived from the light absorption spectrum by the formula (2)[33]

$$\eta_{LHE} = 1 - 10^{-\mathrm{absorbance}}. \tag{2}$$

It is easy to obtain according to Fig. 2 that Mn-doped photoanodes have larger light harvesting efficiency η_{LHE}. Charge injection efficiency η_{Inj} determined by the stepped band structure.[34] According to the theoretical calculation results, the Mn doping does not change the position of the conduction band, and thus does not affect the charge injection efficiency η_{Inj}. As for the charge collection efficiency η_{cc}, it

mainly depends on the charge recombination in the entire device. According to the dark current of devices as shown in Fig. 5(a), the Mn-doped sample can effectively suppress the charge recombination and promote the separation of photogenerated carriers. This is because the Mn ions increase the valence band top energy of ZnSe and promote the transport of holes from the quantum dots to the electrolyte, so electron hole recombination is reduced.[22] Based on the above analysis, Mn doping improves the light harvesting efficiency η_{LHE} and charge collection efficiency η_{cc}, thereby enhancing the IPCE and ultimately the PCE of the solar cell is significantly improved.

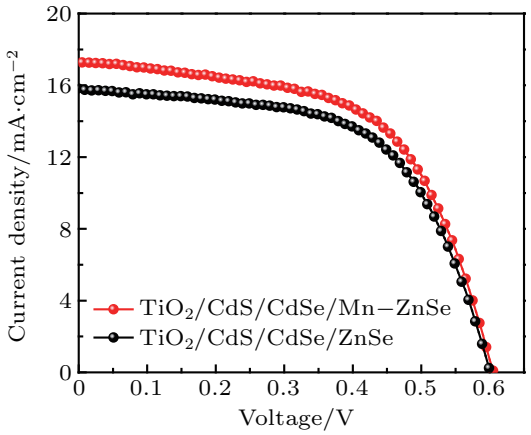


Fig. 6. Current density–voltage (J–V) characteristics of the QDSSCs with ZnSe and Mn-doped ZnSe as a passivation layer.

Table 1. Photoelectric parameters of QDSSCs.

Sample	V_{oc}/V	J_{sc}/mA·cm^{-2}	FF	η/%
TiO$_2$/CdS/CdSe/ZnSe	0.60	15.71	0.59	5.62
TiO$_2$/CdS/CdSe/Mn–ZnSe	0.61	17.29	0.58	6.12

Figure 6 shows the J–V curve of ZnSe and Mn-doped ZnSe samples. The detailed parameters of the J–V test are listed in Table 1. It is found in Table 1 that the introduction of Mn ions does not change the open circuit voltage (V_{oc}) and fill factor (FF) of devices. This is because the V_{oc} of QDSSCs is mainly determined by the energy band position of the CdS/CdSe quantum dots and the redox potential of the electrolyte.[35] Obviously, Mn-doped ZnSe significantly improved the short-circuit current J_{sc} of the device, and the J_{sc} value of the solar cell increased from 15.71 mA·cm^{-2} to 17.29 mA·cm^{-2} compared with the sample without manganese doping. The main reason is that Mn doping broadens the light absorption range of solar cells and reduces interfacial recombination, resulting in the final PCE of 6.12% for QDSSCs, an increase of 9%.

4. Conclusion

According to a series of experimental characterization and theoretical analysis, it can be concluded that the use of Mn-doped ZnSe as a passivation layer on the surface of TiO$_2$/CdS/CdSe co-sensitized solar cells can effectively improve the PCE of solar cells. The introduction of more porous membrane structure increases light reflection and improves the utilization ratio of light, thus enhancing the light absorption intensity. Meanwhile, the valence band of the Mn-doped ZnSe passivation layer is shifted upward compared to the pure ZnSe passivation layer, which results in red-shift of light absorption edge and promote hole transport of QDSSCs, suppressing charge recombination. Finally, QDSSCs with Mn-doped ZnSe as a passivation layer achieved a power conversion efficiency PCE of 6.12%, an increase of 9% compared to a device without manganese doping (5.62%). This work system explains the effect of Mn-doped ZnSe passivation layer for high-performance CdS/CdSe QDSSCs.

Appendix A: Supporting information

The atomic percentages of EDX, combined with the EDX spectra of TiO$_2$/QDs/ZnSe samples are given in the following table and figures.

Table A1. The atomic percentages of the main elements in photoanodes.

Sample	O	Ti	S	Cd	Zn	Se	Mn
TiO$_2$/CdS/CdSe/ZnSe	55.06	28.41	6.76	5.23	3.11	2.53	–
TiO$_2$/CdS/CdSe/Mn-ZnSe	45.22	30.03	7.49	6.58	6.31	3.08	1.29

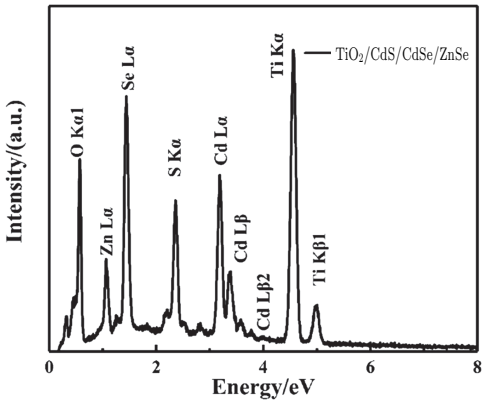


Fig. A1. Energy dispersive x-ray spectrum of TiO$_2$/CdS/CdSe/ZnSe.

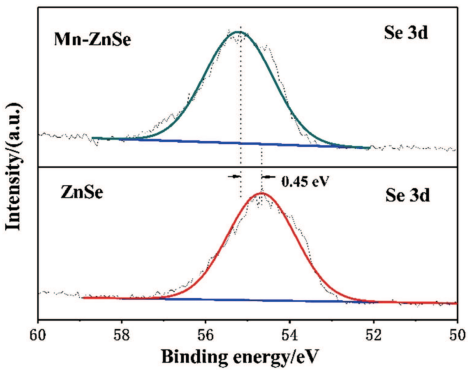


Fig. A2. The XPS spectra of Se with and without manganese doping.

References

[1] Holdren. J P 2008 *Science* **319** 424
[2] Verma S, Kaniyankandy S and Ghosh H 2013 *J. Phys. Chem. C* **117** 10901
[3] Pan Z, Rao H, Mora-Sero I, Bisquert J and Zhong X 2018 *Chem. Soc. Rev.* **47** 7659
[4] Gu Y, Tang L B, Guo X P, Xiang J Z, Teng K S and Liu S P 2019 *Chin. Phys. B* **28** 047803
[5] Tian J and Cao G 2015 *J. Phys. Chem. Lett.* **6** 1859
[6] Wang J, Li Y and Shen Q 2016 *J. Mater. Chem. A* **4** 877
[7] Wu W Q, Xu Y F, Chen H Y, Kuang D B and Su C Y 2019 *Acc. Chem. Res.* **52** 633
[8] Dong J, Xu X, Shi J J, Li D M, Luo Y H, Meng Q B and Chen Q 2015 *Chin. Phys. Lett.* **32** 078401
[9] Huang J, Xu B, Yuan C Z, Chen H, Sun J L, Sun L C and Agren H 2014 *ACS Appl. Mater. Interfaces* **6** 18808
[10] Hou J, Zhao H, Huang F, Chen L, Wu Q, Liu Z, Peng S L, Wang N and Cao G Z 2018 *J. Mater. Chem. A* **6** 9866
[11] Xu Y F, Wu W Q, Rao H S, Chen H Y, Kuang D B and Su C Y 2015 *Nano Energy* **11** 621
[12] Li K Y, Ren L and Shen T D 2018 *Chin. Phys. B* **27** 067305
[13] Huang F, Hou J and Zhang Q 2016 *Nano Energy* **26** 114
[14] Trepyow A and Nix F C 1939 *JOSA* **29** 457
[15] Shen T, Tian J, Lv L, Fei C, Wang Y, Pullerits T and Cao G 2016 *Electrochim. Acta* **191** 62
[16] Horoz S, Dai Q, Maoney F and Tang J 2015 *Phys. Rev. Appl.* **3** 024011
[17] Gou X, Dong H, Niu G, Qiu Y and Wang L 2014 *RSC. Adv.* **4** 21294
[18] Wu Z M, Wang W P, Cao Y Y, He J L, Luo Q, Bhutto W A, Li S P and Kang J Y 2014 *J. Mater. Chem. A* **2** 14571
[19] Santra P and Kamat P 2012 *J. Am. Chem. Soc.* **134** 2508
[20] Tian J, Lv L, Fei C, Wang Y, Liu X and Cao G Z 2014 *J. Mater. Chem. A* **2** 19653
[21] Wang F, Yang M, Ji S, Yang L, J Zhao J, Liu H, Sui Y, Sun Y, Yang J and Zhang X 2018 *J. Power Sources* **395** 85
[22] Zhang Z, Si M S, Wang Y H, Gao X P, Sung D, Hong S and He J J 2014 *J. Chem. Phys.* **140** 174707
[23] Huang F, Hou J, Zhang Q F, Wang Y, Masse, R C, Peng S L, Wang H L, Liu J S and Cao G Z 2016 *Nano Energy* **26** 114
[24] Zhang Z Y, Xie J F, Yang D Z, Wang Y H, Si M S and Xue D S 2015 *Appl. Phys. Express* **8** 055201
[25] Gopi V V M, Venkata-Haritha M, Soo-Kyoung Kim and Hee-Je Kim 2015 *Nanoscale* **7** 12552
[26] Wang G S, Wei H Y, Luo Y H, Wu H J, Li D M, Zhong X H and Meng Q B 2016 *J. Power Sources* **302** 266
[27] Hoseinzadeh T, Ghoranneviss M, Akbarnejad E and Ghorannevis Z 2018 *Chin. Phys. Lett.* **35** 036101
[28] Dabbousi B O, RodriguezViejo J, Mikulec F V, Heine J R, Mattoussi H, Ober R, Jensen K F and Bawendi M G 1997 *Phys. Chem. B* **101** 9463
[29] Zhang Z Y, Si M S, Peng S L, Zhang F, Wang Y H and Xue D S 2015 *J. Solid State Chem.* **231** 64
[30] Chen X L, Huang B J, Feng Y, Wang P J, Zhang C W and Li P 2015 *RSC Adv.* **5** 106227
[31] Mihalache I, Radoi A, Mihaila M, Munteanu C, Marin A, Danila M, Kusko M and Kusko C 2015 *Electrochim. Acta* **153** 306
[32] Shin S S, Kim J S, Suk J H, Lee K D, Kim D W, Park J H, Cho I S, Hong K S and Kim J Y 2013 *ACS Nano* **7** 1027
[33] Yum J H, Jang S R, Humphry-Baker R, Gratzel M, Cid J J, Torres T and Nazeeruddin M K 2008 *Langmuir* **24** 5636
[34] Huang F, Zhang Q F, Xu B K, Hou J, Wang Y, Masse R C, Peng S L, Liu J S and Cao G Z 2016 *J. Mater. Chem. A* **4** 14773
[35] McDaniel H, Fuke N, Makarov N S, Pietryga J M and Klimov V I 2013 *Nat. Commun.* **4** 2887